Evaluating Seismic Response of Underground Structures Based on the Beam on Dynamic Visco-Elastic Foundation Theory

Alireza Darvishpour Bafroui[1], Ali Ghanbari[2*], and Hamid Zafarani[3]

1. M.Sc. Student, Faculty of Engineering, Kharazmi University, Iran
2. Associate Professor, Faculty of Engineering, Kharazmi University, Iran,
* Corresponding Author; email: ghanbari@khu.ac.ir
3. Assistant Professor, Seismology Research Center, International Institute of Earthquake Engineering and Seismology (IIEES), Iran

Received: 11/06/2011
Accepted: 18/06/2013

ABSTRACT

Underground structures, which are located in seismic zones, should undergo static loads induced by the ground and dynamic earthquake-induced forces. Cross section of the underground structures is usually less than the wavelength of input ground motion. Therefore, semi-static or semi-dynamic methods can be used in cross sectional analysis of these types of structures. In this paper, based on the beam on dynamic visco-elastic foundation theory, a new analytical method was developed to determine the shear deformations of the buried box structures. The proposed method is able to consider the characteristics, such as frequency of the ground motion and the damping ratio, in calculating the seismic displacements, which is less considered in the past analytical methods that was introduced by other researchers. The results of the proposed method indicate that the seismic deformation of underground structures is considerably dependent to damping ratio and frequency of ground motion as well as mechanical and geometrical properties of the surrounding medium and structure. In addition, in some frequencies, the results of the new method indicate good general agreement with the methods developed by other researchers. Nonetheless, according to the effect of the frequency, in some frequencies, remarkable differences are observed.

Keywords:
Underground structures;
Seismic deformation;
Analytical method;
Damping ratio

1. Introduction

Underground structures are usually constructed with high-strength concrete. Structural components of the underground structures should be designed for both static and dynamic seismic loads. Seismic motions or movement of the active faults, which are perpendicular to the structure, causes seismic displacements of the underground structures. In this paper, specifically the displacement caused by seismic motion is considered. Totally, three approaches are used in analysis of the underground structures, which are semi-static, semi-dynamic and dynamic. Generally, the cross sectional area of the underground structures is less than the wavelength of the seismic waves; therefore, semi-static and semi-dynamic methods can be used in their analysis [1].

In addition, there are four main methods for analysis of the underground structures [2], which are mentioned in the following:

1. Dynamic earth pressure method
2. Free field racking deformation method
3. Soil structure interaction method
4. Simplified frame analysis method

The first method is appropriate for the tunnels constructed close to the ground surface. The second one indicates realistic consequences, only if the stiffness of the structure and the surrounding soil are

in similar range. Newmark [3] and Kuesel [4] established a simple method to calculate the free field deformations under the influence of harmonic waves. Totally, using the free field raking method in analysis of the underground structure without considering the soil-structure interaction, can lead to an appropriate initial estimation of the deformations. However, if the stiffness of the soil and the underground structure has remarkable differences, there would be a considerable difference between the real values and the results of this method. Another group of analytical methods considers the soil-structure interaction based on beam on elastic foundation theory. Accordingly, using analytical methods, Penzien and Wu [5], Penzien [6] and Hashash et al. [7] determined the cross sectional deformations of the structure and calculated the loads acting on it. In addition, in soil-structure interaction method, numerical methods such as Wang [8], Pakbaz and Yareev and [9], Liu and Song [10], Kouretzis et al. [11], Shahrour et al. [12] and analytical methods such as Kawashima [13], Penzien and Wu [5], Penzien [6], Hashash et al. [14], Bakhtin [15], Gill et al. [16], Nishioka and Unjoh [17], Bobet [18], Huo et al. [1] are used. In all mentioned analytical methods, the following assumptions are considered:

Penzien [6] and Hashash et al. [7] using beam on elastic foundation theory estimated the magnitude of the forces acting on the cross section of the structure in two full-slip and no-slip states. Nishioka and Unjoh [18] developed an analytical relation for determining the ratio of the shear strain of the structure to the shear modulus of the soil, using the shear strain transmitting characteristics. Besides, by conducting a non-linear analysis, structure-free field shear deformation ratio was evaluated and then, by using the two aforementioned relations, the shear deformations of the structure was determined.

By locating the structure under far field shear and using the elasticity theory, Huo et al. [1] estimated the magnitude and distribution of the shear and normal forces acting on the structure and then the value of shear deformation of the structure was evaluated.

In the present study, an analytical method is developed to estimate the shear deformation of the rectangular underground structures. In the proposed method, the effect of two significant parameters, damping ratio and frequency of input ground motion, as well as soil-structure interaction is considered.

2. Assumptions and Formulation of the Proposed Method

The proposed method is based on beams on dynamic visco-elastic foundation theory. The assumptions of the theory are as follows:

1. The soil assumed to be homogeneous with visco-elastic behavior;
2. The structure is assumed to behave linear elastically;
3. The shear modulus and damping ratio of soil layer assumed to be constant with depth;
4. The roof system assumed to be rigid, to cause uniform deformations in the sides of structure;
5. The structure has rectangular cross section.

According to 4th assumption, the shear stiffness of the structure can be determined using the following equation [20]:

$$\sum_{n=1}^{\infty} \frac{12EI}{L^3} = \frac{24EI}{L^3} \tag{1}$$

where E is Young's modulus for structure material, I is the moment of inertia of columns or walls of structure and L is the structure height.

To simulate the soil-structure interaction, a spring-damper model, as shown in Figure (1), has been used [20]:

$$K_s = 1.2\, E_s \tag{2}$$

where E_s is elasticity modulus of the soil. Hysteretic damping C_m and radiation damping C_r are used for evaluating the damping ratio of soil. Therefore, total damping is defined by Eq. (3). [20]:

$$C = C_m + C_r \tag{3}$$

According to the rectangular cross section of the structure, the radiation-damping ratio can be written

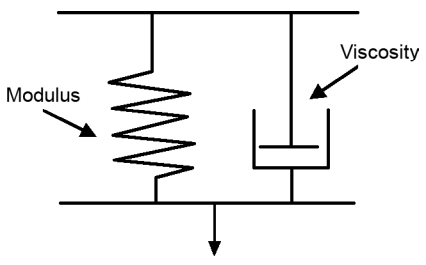

Figure 1. Spring-damper model to simulate soil-structure interaction.

as [21]:

$$\frac{C_r}{\frac{32}{\pi}B\rho_s\nu_s}=\left\{1+\left[\frac{3.4}{\pi(1-\nu)}\right]^{\frac{3}{4}}\right\}\left(\frac{\pi}{4}\right)^{\frac{3}{4}}a_0^{\frac{-1}{4}} \quad (4)$$

where ρ_s is total unit weight of soil, ν is poisson's ratio, a_0 is dimensionless parameter of frequency defined as $\frac{\omega B}{\nu_s}$, ω is vibration frequency, ν_s is shear-wave velocity and B is the square equivalent dimension that represent the area that is perpendicular to structure plane. In addition, Eq. (5) [20] defines the radiation damping.

$$C_m=2k_s\frac{\beta}{\omega} \quad (5)$$

where k_s is soil stiffness and β is the damping ratio. Thus, the Eq. (6) is applied to estimate free-field shear distortions [22]:

$$U_{ff}=U_g\frac{\cos(\delta z)}{\cos(\delta H)} \quad (6)$$

where:

$$\delta=\frac{\omega B}{\nu_s^*}$$
$$\nu_s^*=\nu_s\sqrt{1+2i\beta} \quad (7)$$

U_{ff} is free-field motion of soil, U_g is bedrock motion, δ is wave number, ν_s^* shear wave velocity and β is the damping ratio. Figure (2) represents the comprehensive model of the proposed method. In the next step, considering the assumptions and simulations, the dynamic equilibrium equation for a structural element is defined, Figure (3).

First, the dynamic equilibrium is written in the time domain, Eq. (8).

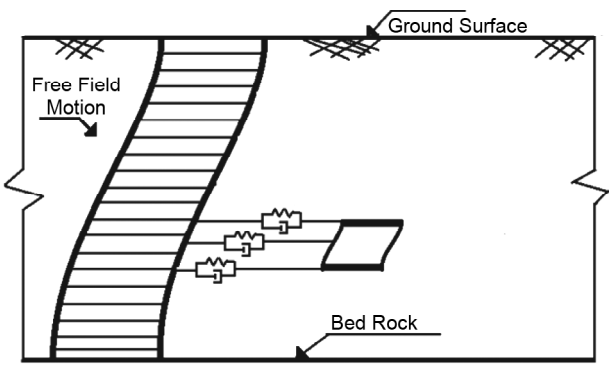

Figure 2. Modeling of the transition of free-field shear motion to the structure by spring-damper system.

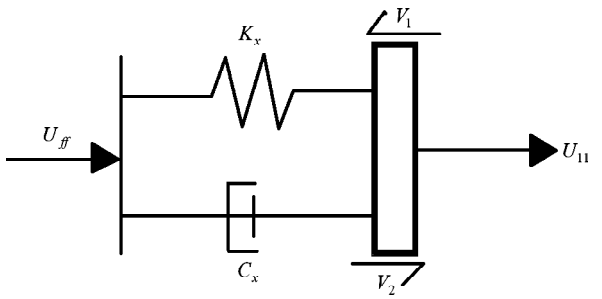

Figure 3. Dynamic equilibrium equation for a structural element.

$$K_x(U_{11}-U_{ff})+C_c(\dot{U}_{11}-\dot{U}_{ff})+\Delta V+m\ddot{U}_{11}=0 \quad (8)$$

Then, the equation can be written as follows in the frequency domain, Eq. (9):

$$K_x(U_{11}-U_{ff})e^{i\omega t}+C_x(U_{11}-U_{ff})i\omega e^{i\omega t}+\Delta V+mU_{11}(-\omega^2)e^{i\omega t}=0 \quad (9)$$

Afterward, Eq. (9) is divided by $e^{i\omega t}$ and is re-written in the following form, Eq. (10):

$$\frac{\Delta V}{e^{i\omega t}}+(K_x+i\omega C_x-m\omega^2)U_{11}=(K_x+i\omega C_x)U_{ff} \quad (10)$$

In this step, according to the stiffness of the simulated structure Eq. (10) is rearranged as follows:

$$\frac{24EI}{L^3}\frac{d^4U_{11}}{dz^4}+(k_x+i\omega c_x-m\omega^2)U_{11}=(k_x+i\omega c_x)U_g\frac{\cos\delta z}{\cos\delta H} \quad (11)$$

where E is the elasticity modulus, I is the moment of inertia, L is the structure height and H is the soil layer height. Eq. (11) is a fourth-order differential equation that needs independent boundary conditions to be solved. These boundary conditions are mentioned hereunder:

The roof of the structure assumed to be rigid, so we have:

$$\frac{dU_{11}}{dz}(h_1)=0 \quad (12)$$

where $\frac{dU_{11}}{dz}$ is first order derivative of U_{11}, which represents the structure deformation versus height (z).

In addition, the bottom of the structure assumed to be rigid, so:

$$\frac{dU_{11}}{dz}(h_1+L)=0 \quad (13)$$

Shear force that was induced in the roof of system is written as follows:

$$\frac{d^3U_{11}}{dz^3}(h_1) = -V_1 \tag{14}$$

where the Eq. (15) [21] determines V_1 as:

$$V_1 = (1-0.15h_1)\frac{a}{g}\gamma h_1 \tag{15}$$

where h_1 is the thickness of soil layer on the structure, γ is unit weight of the soil, a represents the ratio of acceleration to the base acceleration, and b is the structure width.

Eq. (16) also defines shear force induced in the bottom of structure:

$$\frac{d^3U_{11}}{dz^3}(h_1+L) = -V_2 \tag{16}$$

where V_2 is:

$$V_2 = (1-0.15(h_1+L))\frac{a}{g}\gamma(h_1+L)b \tag{17}$$

Now, using four mentioned boundary conditions, the Eq. (11) can be solved. First, the complementary solution is found by considering the homogeneous differential equation, which is represented in Eq. (18).

$$\frac{24EI}{L^3}\frac{d^4U_{11}}{dz^4} + (k_x + i\omega c_x - m\omega^2)U_{11} = 0 \tag{18}$$

Then, the complementary solution of the Eq. (18) is determined using Eq. (19).

$$U_c = Ae^{\lambda z} + Be^{-\lambda z} + Ce^{i\lambda z} + De^{-i\lambda z} \tag{19}$$

where:

$$\lambda = \left\{\frac{L_3}{24EI}(m\omega^2 - i\omega c_x - k_x)\right\}^{\frac{1}{4}} \tag{20}$$

The particular solution of the equation is obtained by an operator method. Eq. 21 indicates the particular solution.

$$U_p = \frac{(k_x + i\omega c_x)U_g}{(\frac{24EI}{L_3}\delta^4 + k_x + i\omega c_x - m\omega^2)}\frac{\cos\delta z}{\cos\delta H} \tag{21}$$

Therefore, total solution of the Eq. (18), which is the sum of the complementary and particular solutions, can be written as Eq. (22):

$$U_{11} = Ae^{\lambda z} + Be^{-\lambda z} + Ce^{i\lambda z} + De^{-i\lambda z} + \frac{(k_x + i\omega c_x)U_g}{(\frac{24EI}{L_3}\delta^4 + k_x + i\omega c_x - m\omega^2)}\frac{\cos\delta z}{\cos\delta H} \tag{22}$$

where A, B, C and D are equation constants and the following system of equations should be solved to evaluate their values. Eq. (23) was developed using four boundary conditions:

$$\begin{bmatrix} \lambda e^{\lambda h1} & -\lambda e^{-\lambda h1} \\ \lambda e^{\lambda(h1+L)} & -\lambda e^{-\lambda(h1+L)} \\ \frac{24EI}{L_3}\lambda^3 e^{\lambda h1} & -\frac{24EI}{L_3}\lambda^3 e^{-\lambda h1} \\ \frac{24EI}{L_3}\lambda^3 e^{\lambda(h1+L)} & \frac{24EI}{L_3}\lambda^3 e^{-\lambda(h1+L)} \end{bmatrix}$$

$$\begin{bmatrix} i\lambda e^{i\lambda h1} & -i\lambda e^{-i\lambda h1} \\ i\lambda e^{i\lambda(h1+L)} & -i\lambda e^{-i\lambda(h1+L)} \\ -\frac{24EI}{L_3}\lambda^3 e^{i\lambda h1} & -\frac{24EI}{L_3}i\lambda^3 e^{-i\lambda h1} \\ -\frac{24EI}{L^3}i\lambda^3 e^{i\lambda(h1+L)} & -\frac{24EI}{L^3}i\lambda^3 e^{-i\lambda(h1+L)} \end{bmatrix}\begin{bmatrix} A \\ B \\ C \\ D \end{bmatrix} \tag{23}$$

$$= \begin{bmatrix} S\delta\sin\delta h1 \\ S\delta\sin\delta(h1+L) \\ -\frac{24EI}{L^3}S\delta^3\sin(\delta h1) - (1-0.15h1)\frac{a}{g}\gamma h1b \\ -\frac{24EI}{L^3}S\delta^3\sin\delta(h1+L) - (1-0.15(h1+L))\times \\ \frac{a}{g}\gamma(h1+L)b \end{bmatrix}$$

4. Results Obtained with the Proposed Method

The formulation of the proposed method was introduced in the former section. In the proposed equation, unlike the equations of other past researchers, the frequency of input ground motion and the damping ratio is also considered. To simplify the considerations, most of diagrams that are represented in this section, are exhibited in $\frac{\Delta_{structure}}{\Delta_{Freefield}}$.

where $\Delta_{structure}$ is shear deformation of structure and $\Delta_{Freefield}$ is free-field shear deformation. Shear deformation of the structure and dimensions, and geometrical properties of the soil layers are shown in Figures (4) and (5). Past researchers used Flexibility ratio to present their results. Flexibility ratio is an index, which represents the ground-structure stiffness ratio [8]. The flexibility ratio is calculated

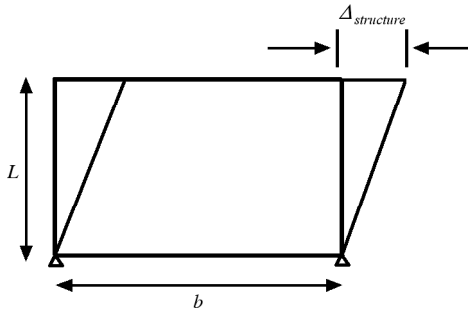

Figure 4. Shear deformation of the structure.

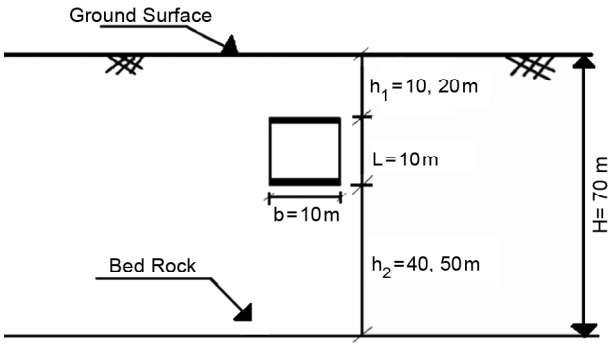

Figure 5. Dimensions and geometrical properties of the soil layers and structure

Table 1. Specifications of the selected soils.

Soil	G_s (kPa)	ν_s (m/s)	ν	β	γ (kN/m^3)
1	20000	100	0.3	0.05	18.614
2	320000	400	0.3	0.05	19.614
3	1280000	800	0.3	0.05	19.812
4	2000000	1000	0.3	0.05	20

Table 2. Specifications of the selected structures.

Structure	t (m)	I (m^4)	B (m)	L (m)	m (Kg)
1	0.5	0.022	10	10	1200
2	0.7	0.0286	10	10	1680
3	0.9	0.0607	10	10	2160
4	1.1	0.111	10	10	2640
5	1.3	0.1831	10	10	3120
6	1.5	0.2813	10	10	3600
7	1.7	0.4094	10	10	4080
8	1.9	0.572	10	10	4560
9	2.1	0.772	10	10	5040
10	2.3	1.0139	10	10	5520
11	2.5	1.302	10	10	6000
12	2.7	1.640	10	10	6480
13	2.9	2.032	10	10	6960
14	3.1	2.483	10	10	7440

m is Mass Per Unit Length

using the following equation:

$$F = \frac{G}{24}\left(\frac{L^2 b}{EI} + \frac{Lb^2}{EI_R}\right) \tag{24}$$

where I_R is the moment of inertia of the roof and bottom of the structure, E is the elasticity modulus, b is the structure width, G is shear modulus of the soil and L is the structure height. Four types of soil and several types of structure with different stiffness and masses where used in the analysis. Tables (1) and (2) represent the properties of the chosen soils and structures, respectively. In addition, structures with higher stiffness modulus are considered in analysis, when the third and fourth types of soil are used.

In this section, due to the importance of the first mode of vibration, only frequencies are considered that their input wavelength is less than height of the structure. The resonance frequency, which is the frequency that maximum deformations occur in the structure, can be calculated using the Eq. (25) [21].

$$\omega = \frac{\pi V_s}{2H} \tag{25}$$

where V_s is the shear wave velocity and ω is input wave frequency.

Figures (6) to (8) indicate the structure - free field deformation ratio versus the flexibility ratio, for different frequencies and types of soil. In addition, it should be noted that the resonance frequencies that are equal to natural frequencies for a 70-meter thick soil layer is 2.244, 8.976, 17.952 and 22.44 for the soil types 1 to 4, respectively.

As seen in Figure (7), when the frequency is 5 rad/sec, the seismic response of structure has little variations and is very close to soil deformations. This phenomenon happens only in low frequencies. Totally, the less is the frequency; the deformation of structure is closer to the free-field deformation. For instance, in second type of soil when the frequency is 1 rad/sec, the deformations of the soil and the structure are almost the same.

In the following, the variations of shear deformation of the structure are presented for a constant flexibility ratio. Figures (9) to (11) indicate the variation of structure deformation versus the resonance frequency. As can be seen, aforementioned curves have a peak point that refers to the resonance frequency of the soil layer. The third type of soil was used in these diagrams, which has 17.952 rad/sec resonance frequency.

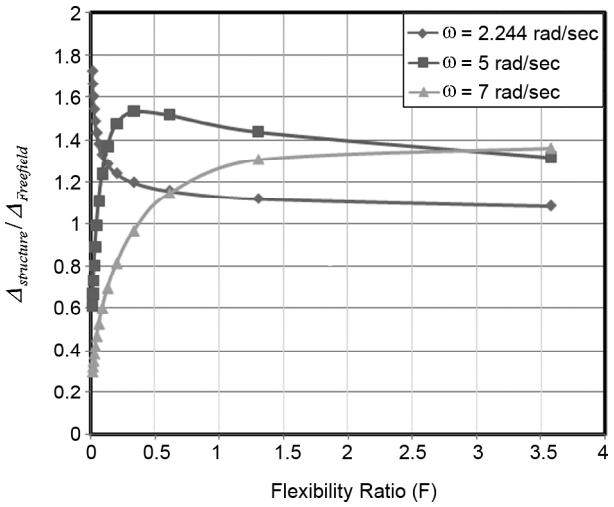

Figure 6. The effect of input wave frequency on the seismic response of structure in first type of soil.

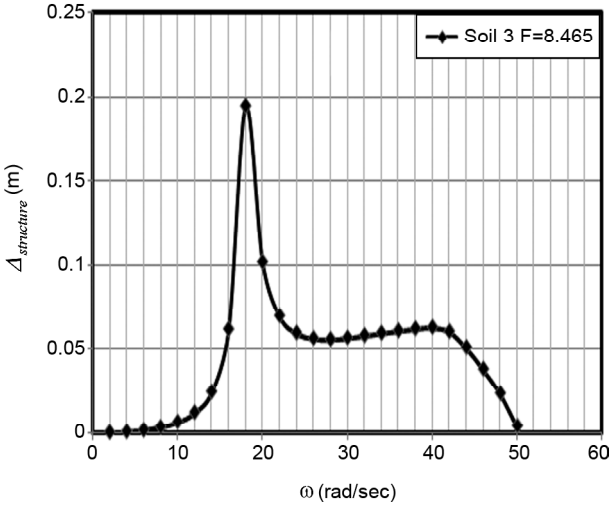

Figure 9. Shear deformation of the structure versus frequency, in constant flexibility ratio (8.465).

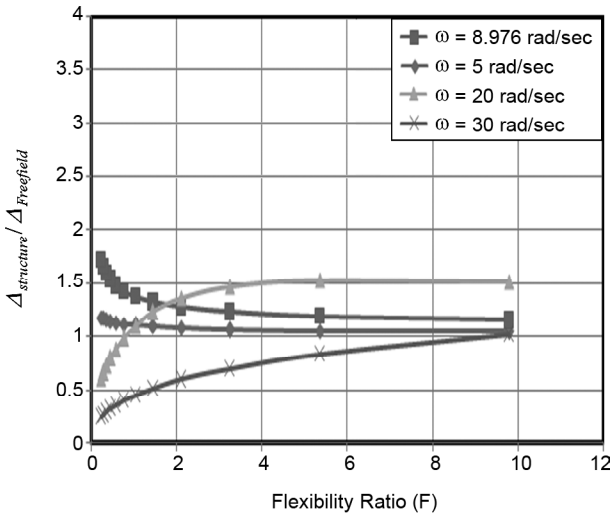

Figure 7. The variations of the structure-free field deformation ratio in second type of soil.

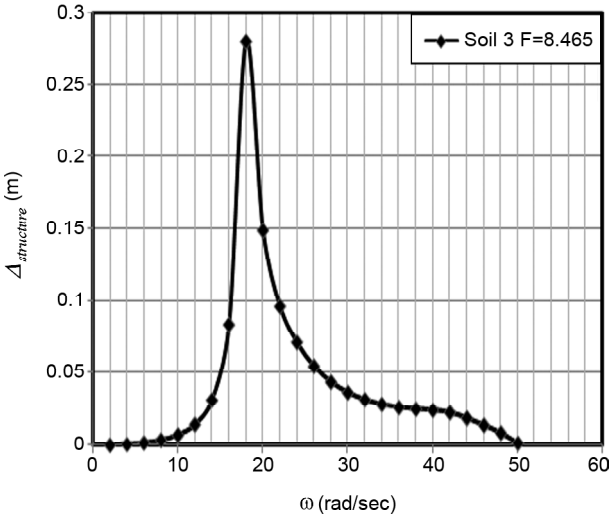

Figure 10. Shear deformation of the structure versus frequency, in constant flexibility ratio (0.666).

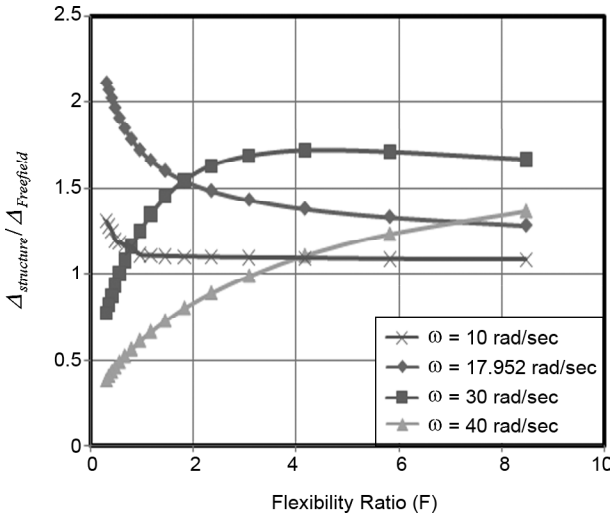

Figure 8. The variations of the structure-free field deformation ratio in third type of soill.

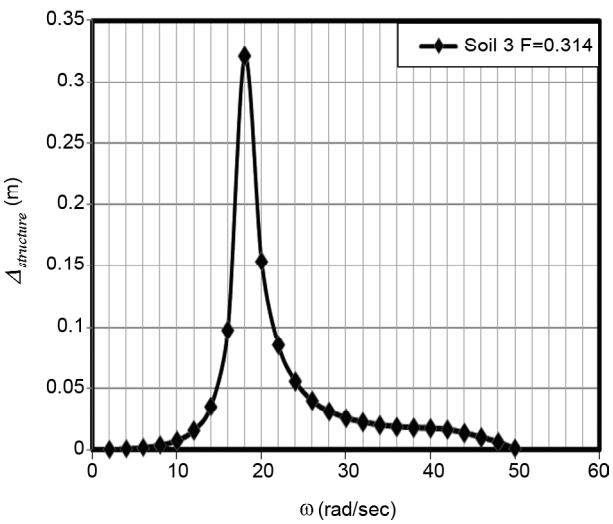

Figure 11. Shear deformation of the structure versus frequency, in constant flexibility ratio (0.314).

Figure (12) represents the comparison of the three former curves, and Figure (13) represents the structure - free field deformation ratio versus frequency. When the frequency is less than resonance frequency or is just a little higher than it, the higher is the stiffness, the higher is the deformation of structure. However, for the frequencies higher than the mentioned range, the inverse relation observed in stiffness and deformation of structure.

As indicated before, for the frequencies less than the resonance frequency, the shear deformation of structure increase with the increase of the stiffness ratio of structure to soil; but, in higher frequencies, the mentioned value decrease with the increase of stiffness. In analytical equations developed by past researchers, damping ratio is less considered. However, in the proposed method, the mentioned parameter is taken into consideration. Figure (14) shows the variation of the seismic response versus damping ratio for the second type of soil. As seen in Figure (14), the seismic response of structure decreased with the increase of damping ratio.

The effect of Poisson's ratio on the seismic response of structure has been surveyed in Figure (15). The results indicate that there is a considerable decrease in structure response with the increase of Poisson's ratio. The results are identical to the results obtained by Penzien analytical method [6].

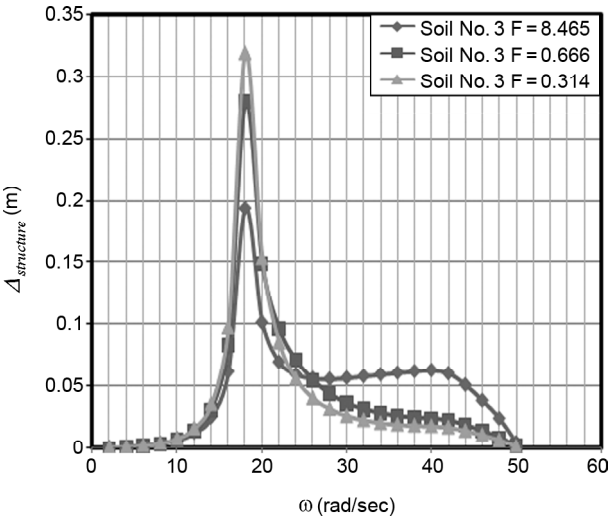

Figure 12. Variations of the shear deformation of structure versus frequency.

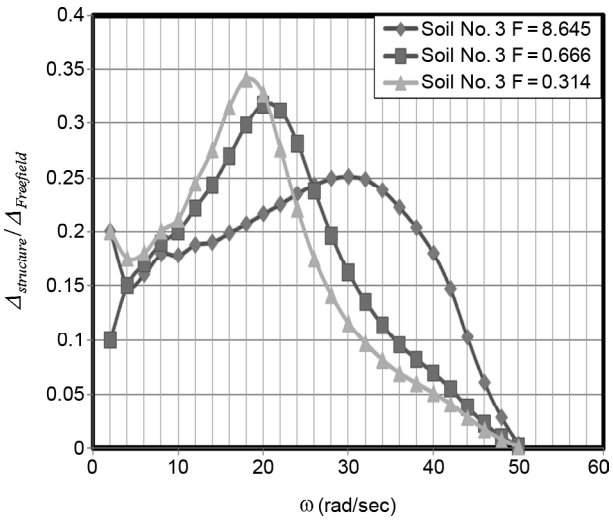

Figure 13. Variations of the structure-free field shear deformation ratio versus frequency of ground motion.

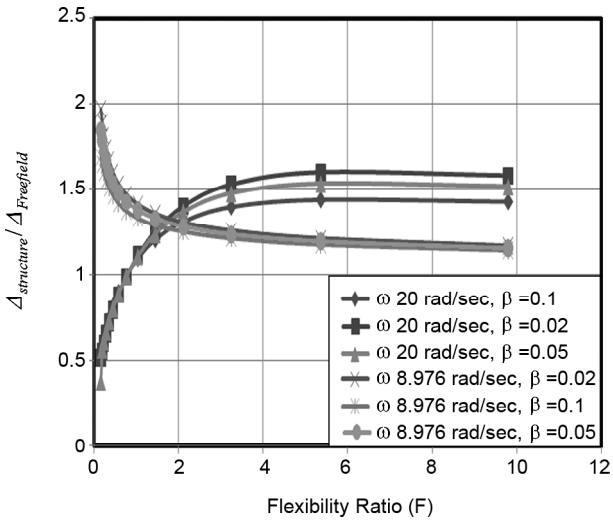

Figure 14. Variation of the structure-free field deformation ratio in the second type of soil at different frequencies and damping ratios

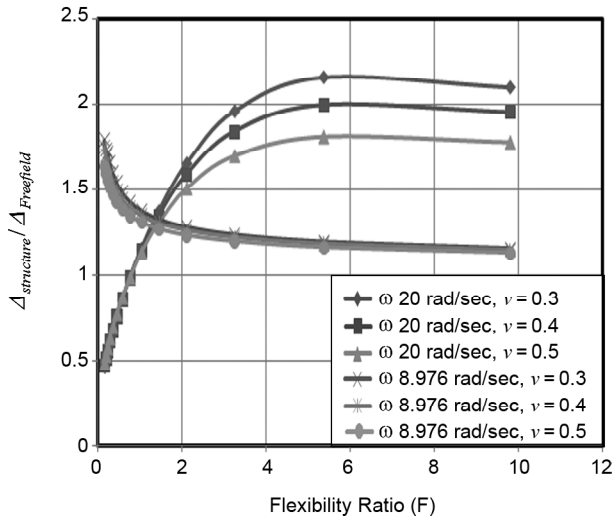

Figure 15. Variation of the structure-free field deformation ratio in the second type of soil at different frequencies and Poisson's ratios.

5. Verification of the Analytical Solution

In the following section, the results of the proposed method are compared to the other past analytical methods. Furthermore, the results are compared to the output results of the Quake/W (2007) software. QUAKE/W is a geotechnical finite element software product for the dynamic analysis of earth structures subjected to earthquake shaking, or point dynamic forces from a blast or a sudden impact load.

Table (3) represents the results of the proposed method for four chosen types of soil in different flexibility ratios, in comparison with that obtained from the simulations in Quake/W (2007).

Mostly, both analytical and simulation results indicate similar procedure. Nevertheless, quantitatively, the results of the proposed method are almost identical to the output of software in some frequencies. However, in other frequencies, up to 25 percent difference is observed.

Wang [8] conducted series of numerical analysis on different types of the rectangular underground structures, and presented diagrams for the structure-free field shear deformation ratio versus flexibility ratio. The results of the proposed method are compared to that of Wang method in Figure (16). Accordingly, the structure-free field shear deformation ratio varies with changes in type of soil and frequency. In third type of soil, at a constant frequency (30 rad/sec), the structure-soil deformation ratio obtained by the proposed method is higher than that of Wang [8] method until the flexibility ratio is less than four. Nevertheless, for higher flexibility ratios, the results of Wang method are higher than that of proposed method. In addition, in second type of soil, at 20 rad/sec frequency, the results of the proposed method are higher than Wang [8] method until the flexibility ratio is less than two and for higher flexibility ratios, the reverse is true.

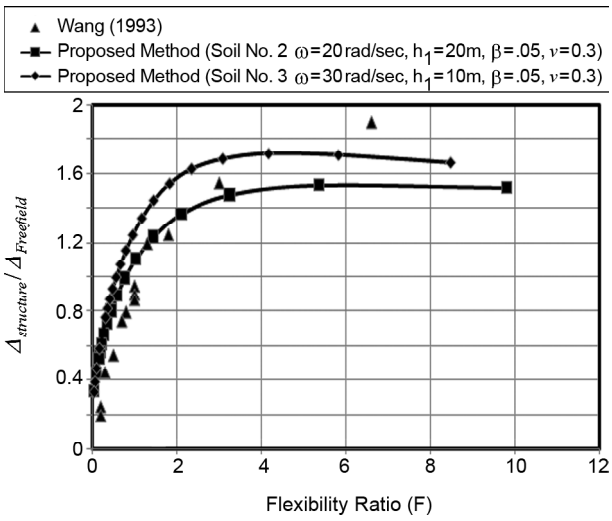

Figure 16. Comparison of the results of the proposed analytical method and Wang (1993) method.

Penzien [6], based on beam on elastic foundation theory, established analytical method to investigate the structure-free field shear deformation versus flexibility ratio. Figures (17) to (20) represent the comparison of the results of the proposed method to the results obtained by Penzien [6] method. The same procedure was observed in both methods. Nevertheless, because the Penzien [6] method is frequency-independent, its results are among the results obtained by proposed method. In addition, it should be noted that when the structure stiffness is higher than the soil stiffness, Penzien [6] method

Table 3. Comparison of the results of the proposed method to the outputs of the Quake/W (2007).

	Soil No. (2)			Soil No. (3)			Soil No. (4)			Soil No. (4)		
	ω = 20 rad/sec			ω = rad/sec			ω = 35 rad/sec			ω = 40 rad/sec		
Flexibility Ratio)	Δ_{str}/Δ_{ff} Analytical	Δ_{str}/Δ_{ff} Quake/W	Error (%)	Δ_{str}/Δ_{ff} Analytical	Δ_{str}/Δ_{ff} Quake/W	Error (%)	Δ_{str}/Δ_{ff} Analytical	Δ_{str}/Δ_{ff} Quake/W	Error (%)	Δ_{str}/Δ_{ff} Analytical	Δ_{str}/Δ_{ff} Quake/W	Error (%)
8.5	1.52	1.54	1.3	1.5	1.66	9.6						
3.5	1.48	1.47	0.67	1.69	1.35	20	1.75	1.38	21	1.39	1.41	1.4
1.5	1.24	1.2	3.2	1.46	1.17	20	1.46	1.18	19	1.15	1.05	8
1	1.04	1.04	0	1.24	1	19	1.2	1.03	17	0.92	1	8
0.5	0.79	0.83	4.81	0.93	0.76	18	0.95	0.8	15.7	0.68	0.75	9.3
0.3	0.66	0.57	13.6	0.027	0.02	25	0.75	0.6	20	0.51	0.53	3.7

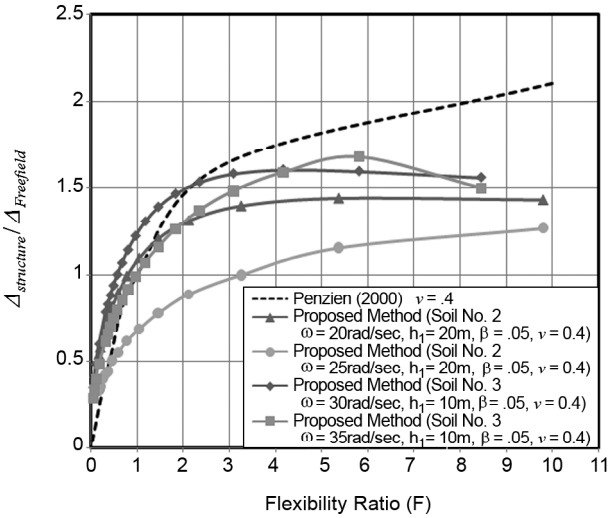

Figure 17. Comparison of the results of the proposed analytical method and Penzien [6] method (υ = 0.4).

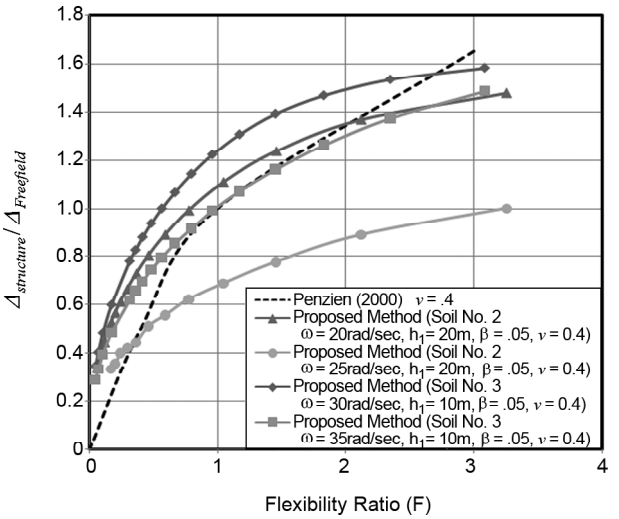

Figure 18. Comparison of the results of the proposed analytical method and Penzien [6] method (υ =0.4 and F<4).

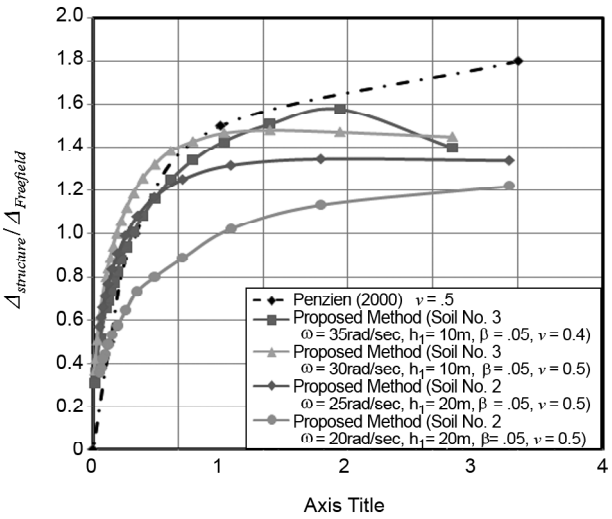

Figure 19. Comparison of the results of the proposed analytical method and Penzien (2000) method (υ =0.5).

always gives higher results.

In Huo et al. [1] method, the structure is under far-field shear stresses and based on the elasticity theory, the amount and distribution of the induced shear forces in rectangular underground structures is determined. Figures (21) and (22) indicate the comparison of the results of the proposed method to the results obtained by Huo et al. [1] method. As seen in these figures, in high flexibility ratios, considerable differences exist between the results, but in low flexibility ratios, the difference is negligible.

On the other hand, to survey the effect of the ground motion frequency on the seismic response, the structure-free-field deformation ratio is also determined for frequencies less than 50 rad/sec.

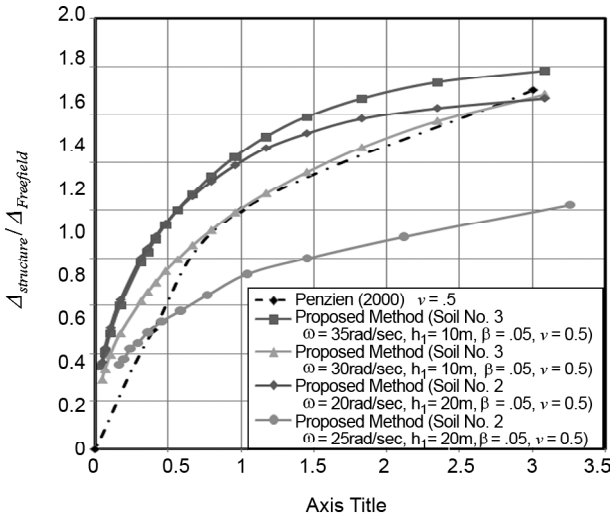

Figure 20. Comparison of the results of the proposed analytical method and Penzien [6] method (υ =0.4 and F<4).

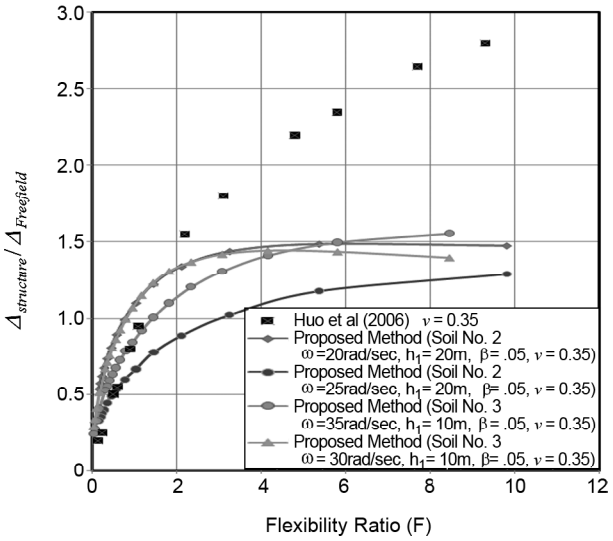

Figure 21. Comparison of the results of the proposed analytical method and Huo et al. [1] method.

Figures (23) to (25) represent the results of the proposed method comparing to the Wang [8] method. The results clarify that the proposed method has the capability to consider the effect of the frequency. Besides, considering the flexibility ratio in a point of the frequency domain, the results of the proposed method are in acceptable agreement with that of Wang [8] method. The same comparison was done for Huo et al. [1] method and the results are represented in Figures (26) to (28).

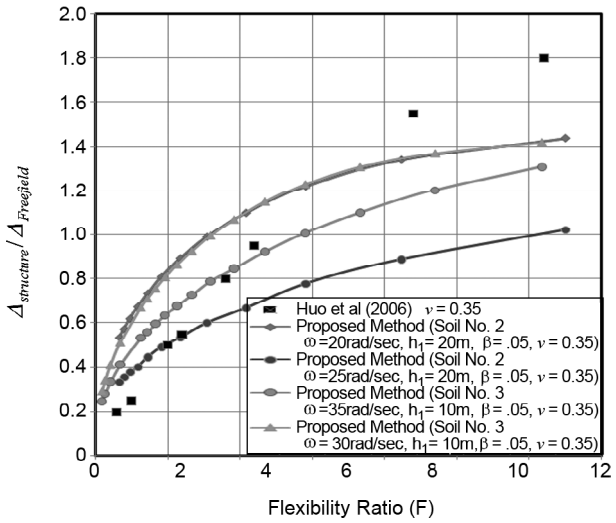

Figure 22. Comparison of the results of the proposed analytical method and Huo et al. [1] method.

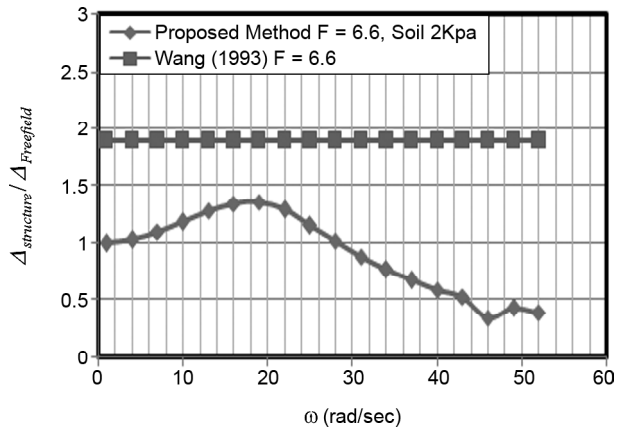

Figure 23. Comparison of the results of the proposed analytical method and Wang [8] method at (F=6.6).

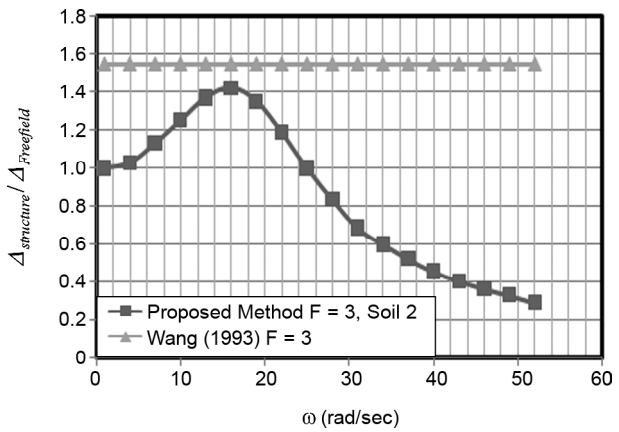

Figure 24. Comparison of the results of the proposed analytical method and Wang [8] method at (F=3).

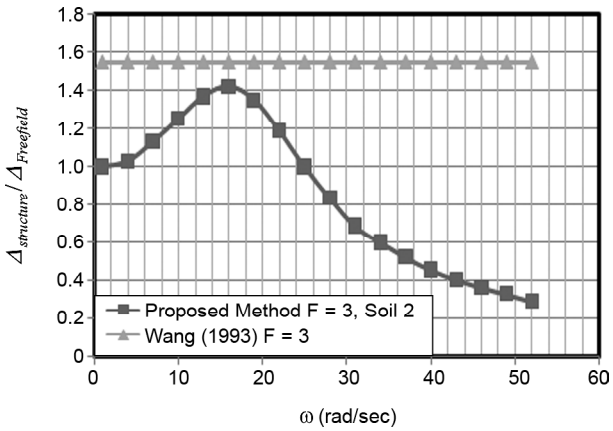

Figure 25. Comparison of the results of the proposed analytical method and Wang [8] method at (F=0.5).

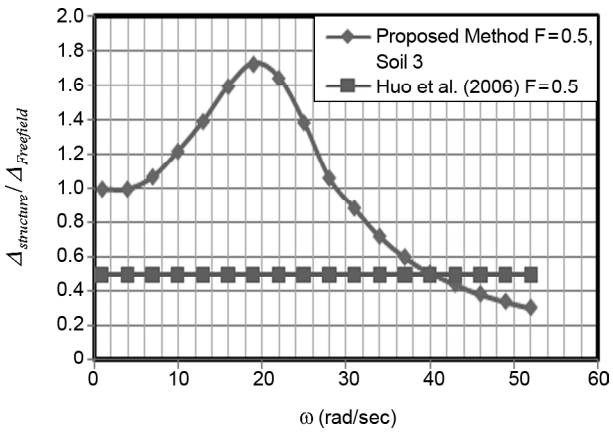

Figure 26. Comparison of the results of the proposed analytical method and Huo et al. [1] method at (F=0.5).

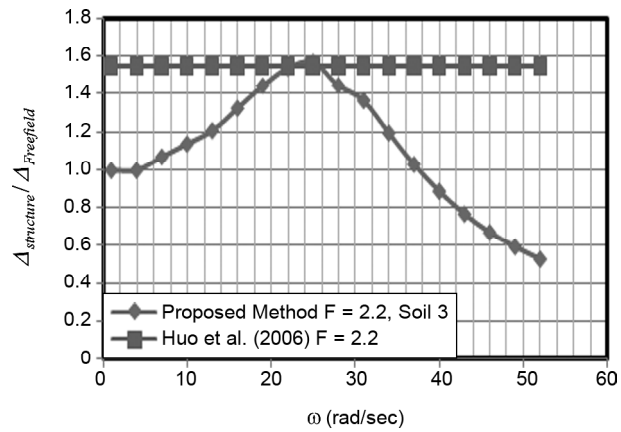

Figure 27. Comparison of the results of the proposed analytical method and Huo et al. [1] method at (F=2.2).

Figures (29) and (30) indicate the variations of seismic response versus damping ratio. As seen in these figures, the higher is the damping ratio, the less is the shear deformation. However, in other methods, the variation of shear deformation is independent of the damping ratio.

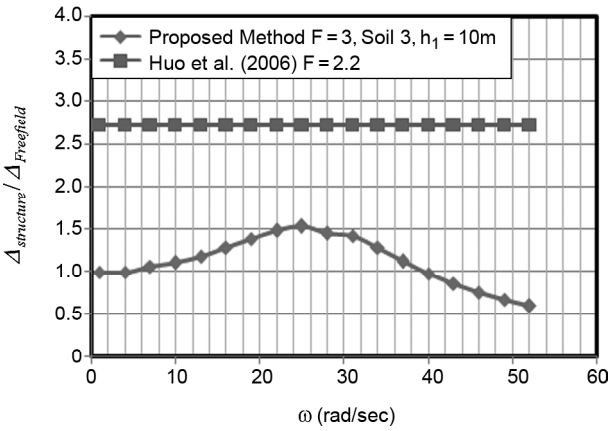

Figure 28. Comparison of the results of the proposed analytical method and Huo et al. [1] method at (F=3).

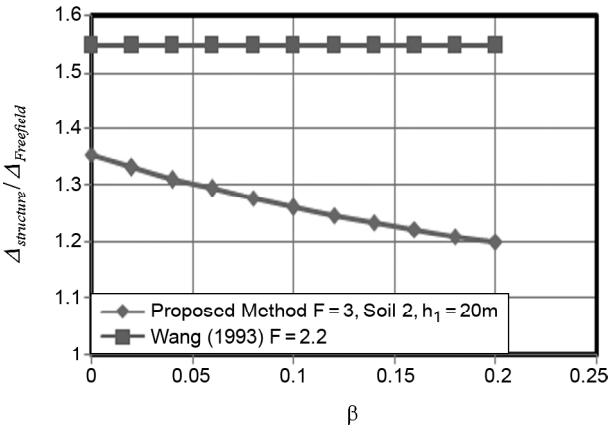

Figure 29. Comparison of the results of the proposed analytical method and Huo et al. [1] method.

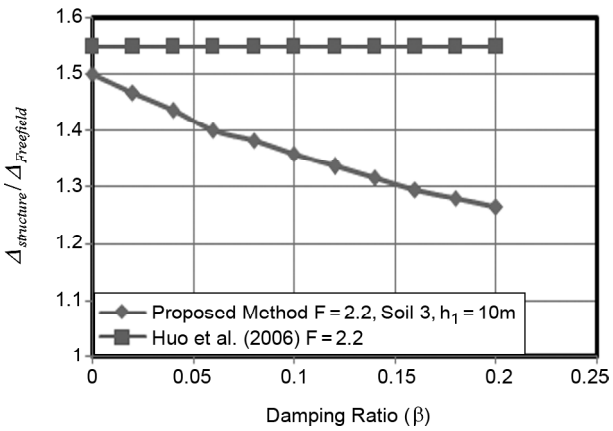

Figure 30. Comparison of the results of the proposed analytical method and Huo et al. [1] method.

In Tables (4) to (7), the results error was detected in comparison to the results of the Quake/W software, for proposed Wang [8] and Huo et al. [1] methods. In most cases, the results of the proposed method indicate a better agreement with the results of the numerical simulations by Quake/W.

Table 4. Comparison of the results of the Wang [8] method, proposed method and numerical simulations (in the second type of soil).

	Proposed Method	**Wang [8]**	**Quake/W (2007)**	**Proposed Method**	**Wang [8]**
F	Δ_{str}/Δ_{ff}	Δ_{str}/Δ_{ff}	Δ_{str}/Δ_{ff}	Error (%)	Error (%)
3.5	1.48	1.6	1.47	0.67	12.5
1.5	1.24	1.21	1.2	3.2	0.82
1	1.04	0.9	1.04	0	13.46
0.5	0.79	0.55	0.83	4.81	34
0.3	0.66	0.45	0.57	13.6	21

Table 5. Comparison of the results of the Wang [8] method, proposed method and numerical simulations (in the second type of soil).

	Proposed Method	**Wang [8]**	**Quake/W (2007)**	**Proposed Method**	**Wang [8]**
F	Δ_{str}/Δ_{ff}	Δ_{str}/Δ_{ff}	Δ_{str}/Δ_{ff}	Error (%)	Error (%)
3.5	1.39	1.6	1.41	1.4	11.8
1.5	1.15	1.21	1.05	8	13.22
1	0.92	0.9	1	8	10
0.5	0.68	0.55	0.75	9.3	27
0.3	0.51	0.45	0.53	3.7	15

Table 6. Comparison of the results of the Huo et al. [1] method, proposed method and numerical simulations (in the second type of soil).

	Proposed Method	**Huo et al. [1]**	**Quake/W (2007)**	**Proposed Method**	**Huo et al. [1]**
F	Δ_{str}/Δ_{ff}	Δ_{str}/Δ_{ff}	Δ_{str}/Δ_{ff}	Error (%)	Error (%)
3.5	1.46	2	1.45	0.68	27.5
1.5	1.22	1.35	1.19	2.45	11.6
1	1.03	0.9	1.02	0.97	11.7
0.5	0.77	0.5	0.8	3.7	37.5
0.3	0.64	0.3	0.55	14	45

Table 7. Comparison of the results of the Huo et al. [1] method, proposed method and numerical simulations (in the fourth type of soil).

	Proposed Method	Huo et al. [1]	Quake/W (2007)	Proposed Method	Huo et al. [1]
F	Δ_{str}/Δ_{ff}	Δ_{str}/Δ_{ff}	Δ_{str}/Δ_{ff}	Error (%)	Error (%)
3.5	1.37	2	1.4	2.1	30
1.5	1.13	1.35	1.04	8	22
1	0.9	0.9	0.98	8	8
0.5	0.65	0.5	0.72	10	30
0.3	0.48	0.3	0.51	5	41

6. Conclusion

In this paper, based on beam on elastic foundation theory, a new analytical method was developed to determine the seismic deformations of the underground structures. The new proposed method is capable to simulate various characteristics of the ground motion and the surrounding medium. Comparing the results of the proposed method with other methods and with the results of the numerical simulations by Quake/W indicate that the new proposed method has less error. In addition, the method can excellently simulate the variation of the ground motion frequency and damping ratio. Furthermore, the results indicate that the frequency of ground motion plays an important role in seismic response of underground structures. As in a constant flexibility ratio, the shear deformation of structure varies with the variations of the ground motion frequency. Nevertheless, in methods proposed by other past researchers, in a constant flexibility ratio, the shear deformation of the structure is frequency-independent.

Besides, in the proposed method, the damping ratio has a considerable effect on the seismic response of the underground structure. While keeping the flexibility ratio constant, the shear deformation decreases with the increase of the damping ratio. In addition, the results indicate that an increase in Poisson's ratio leads to a decrease of the structure-free-field deformation ratio. The dimensions of the structure have a negligible effect on the seismic response of the underground structure.

Consequences imply that the maximum error in the proposed method is about 25 percent, which only occurred in some frequencies. For instance, in third type of the soil, at 30 rad/sec, the maximum observed error is 25 percent, but in the second type of soil, at 20 rad/sec frequency, the maximum and minimum errors are 13 and 0 percents, respectively.

References

1. Huo, H., Bobet, A., Fernandez, G., and Ramirez, J. (2006). Analytical Solution for Deep Rectangular Structures Subjected to Far-Field Shear Stresses, *Tunnelling and Underground Space Technology*, **21**(6), 613-625.
2. FHWA (2005). Seismic Analysis of Retaining Walls, Buried Structures, Embankments, and Integral Abutments, FHWA-NJ-2005-002, 1-160.
3. Newmark, N.M. (1968). Problems in Wave Propagation in Soil and Rock. Proceedings of the International Symposium on Wave Propagation and Dynamic Properties of Earth Materials.
4. Kuesel, T.R. (1969). Earthquake Design Criteria for Subway, *Journal Of Structural Division, ASCE*, **95**(ST6), 1213-1231.
5. Penzien, J. and Wu, C. (1998). Stresses in Linings of Bored Tunnels, *International Journal of Earthquake Engineering and Structural Dynamic*, **27**, 283-300.
6. Penzien, J. (2000). Seismically -Induced Racking of Tunnel Linings, *International Journal of Earthquake Engineering and Structural Dynamic*, **29**(5), 683-691.
7. Hashash, Y.M.A., Hook, J.J., Schmidt, B., and Yao, J.I. (2001). Seismic Design and Analysis of Underground Structures, *Tunnelling and Underground Space Technology*, **16**(4), 247-293.
8. Wang, J.N. (1993). Seismic Design of Tunnels: A State of the Art Approach, Monograph, Monograph 7, Parsons, Brinckerhoff, Quade And Douglas Inc., New York.
9. Pakbaz, C.M. and Yareevand, A. (2005). 2-D Analysis of Circular Tunnels Against Earthquake Loading, *Tunnelling And Underground Space Technology*, **20**(5), 411-417.
10. Liu, H. and Song, E. (2005). Seismic Response of Large Underground Structures in Liquefiable Soils Subjected in Horizontal and Vertical Earth-

quake Excitation, *Computers and Geotechnics*, **32**(4), 223-244.

11. Kouretzis, P.M., Bouckovalas, D.G., and Gantes, J.C. (2006). 3-D Shell Analysis of Cylindrical Underground Structures Under Seismic Shear (S) Wave Action, *Soil Dynamics And Earthquake Engineering*, **26**(10), 909-921.

12. Shahrour, I., Khoshnoudian, M., and Sadek, H. (2010). Elastoplastic Analysis of the Seismic Response of Tunnels in Soft Soils, *Tunnelling and Underground Space Technology*, **25**(4), 478-482.

13. Kawashima, K. (1999). Seismic Design of Underground Structures in Soft Ground, A Review, *Proceedings of the International Symposium on Tunneling in Difficult Ground Conditions*, Tokyo, Japan.

14. Hashash, Y.M.A., Duhee, P., and Yao, J.I. (2005). Ovaling Deformations of Circular Tunnels Under Seismic Loading, an Update on Seismic Design and Analysis of Underground Structures, *Tunnelling and Underground Space Technology*, **20**(5), 435-441.

15. Bakhtin, B.M. (2001). Determining Seismic Loads on Extended Underground Structures, *Hydro Technical Constructions*, **35**(3), 89-93.

16. Gill, M.L., Hernandez, E., and De La Fuente, P. (2001). Simplified Transverse Seismic Analysis of Buried Structures, *Soil Dynamics and Earthquake Engineering*, **21**(8), 735-740.

17. Nishioka, T. and Unjoh, S. (2002). Estimation of the Seismic Shear Deformation of the Underground Structure Based on the Shear Strain Transmitting Characteristics Between Ground and Structure, *JSCE Journal Of Structural Mechanics and Earthquake Engineering*, No. 710, I-60, 273-282.

18. Bobet, A. (2003). Effect of Pore Water Pressure on Tunnel Support During Static and Seismic Loading, *Tunnelling and Underground Space Technology*, **18**(4), 377-393.

19. Chopra, K.A. (1997). Dynamics of Structures: Theory and Applications of Earthquake Engineering Prentice Hall.

20. Gazetas, G. and Dobry, R. (1984). Horizontal Response of Piles in Layered Soils, *Journal of Geotechnical Engineering, ASCE*, **110**(1), 20-40.

21. Kramer, S. (1996). Geotechnical Earthquake Engineering, Prentice-Hall, Upper Saddle River, NJ, USA.